Extended Abstracts of the 2017 International Conference on Solid State Devices and Materials, Sendai, 2017, pp901-902

PS-9-01

# Observation of current-injected Landau-level emission in graphene using a quantum-well based infrared phototransistor

Kazuhiro Takizawa[1], Akira Nishimura[1], Hirokazu Murano[1], Daisuke Nakagawa[1], Kenji Ikushima[1], Sunmi Kim[2], Mikahail Patrashin[3], Iwao Hosako[3], and Susumu Komiyama[3,4]

[1] Department of Applied Physics, Tokyo University of Agriculture and Technology, Koganei, Tokyo 184-8588, Japan
[2]Institute of Industrial Science, The University of Tokyo, Meguro, Tokyo 153-8505, Japan
[3]National Institute of Information and Communications Technology (NICT), Koganei, Tokyo 184-8795, Japan
[4]Department of Basic Science, The University of Tokyo, Meguro, Tokyo 153-8902, Japan

**Abstract**

**Current-injected terahertz (THz) emission from graphene has been observed in high magnetic field. In this experiment, a quantum-well based infrared phototransistor is used for detecting extremely weak Landau-level (LL) emission in monolayer graphene. THz emission takes place when the energy spacing $\Delta E_{\mathrm{LL01}}$ between the zero-energy and the first excited LL ($N = 0 \leftrightarrow N = +1$) is magnetically tuned to a detectable wavelength of 14.5 μm for the phototransistor. The emission efficiency is enhanced when the $eV_{\mathrm{SD}}$ exceeds the $\Delta E_{\mathrm{LL01}}$ and the Fermi level is positioned near the LL filling factor $\nu = +2$, indicating the $N = +1 \rightarrow 0$ inter-LL radiative transition.**

## 1. Introduction

A unique electronic band structure has profound implications for quantum transport in graphene. In particular, monolayer graphene under a perpendicular high magnetic field $B$ forms unequally spaced LLs and an extra LL at the massless Dirac point. In the zero-energy LL of Landau index $N = 0$, some interesting issues peculiar to Dirac particles such as chiral spin edge state or quantum Hall insulator have been suggested [1]. On the other hand, there are theoretical points that the properties of quantum Hall effect (QHE) in actual graphene devices are sensitively characterized by electron (or hole) injection process from metal contacts to the LLs [2].

Measurements of the current-injected LL emission is a powerful method to investigate the nonequilibrium electron dynamics in QHE conductors. In the GaAs-based two-dimensional electron system (2DES), it was possible to study LL emission (a wavelength of about 100 μm) by using single-photon sensitive THz detectors [3]. However, LL emission in graphene has not been observed yet because ultra-sensitive detectors are less developed in the corresponding wavelength (typically 10 - 20 μm in monolayer graphene). In recent year, however, a quantum-well (QW) based charge sensitive infrared phototransistor (CSIP) has been developed in a wavelength range of $\lambda_0 = 12 - 45$ μm [4]. The CSIPs provide an extremely low noise equivalent power, $NEP \sim 7 \times 10^{-20}$ W/H$^{1/2}$, and a high specific detectivity, $D^{*} \sim 1 \times 10^{16}$ cmH$^{1/2}$/W. In this paper, we report the observation of the current-injected THz emission from graphene LLs using the CSIP.

## 2. Experiments

The schematic of the measurement setup is shown in Fig. 1(a). To avoid unintended background infrared radiation, the optical system is embedded into a copper box cooled down to 4.2 K. A monolayer graphene sample is extracted from a bulk graphite crystal and deposited onto $SiO_2$/Si substrate using the standard mechanical method (Fig. 1(b)). The electrodes are fabricated on the sample using electron beam lithography followed by Au/Cr (100/5 nm) evaporation. The CSIP used here is fabricated from a GaAs/AlGaAs triple QW structure, which has the two spectral bands of detection (the wavelength

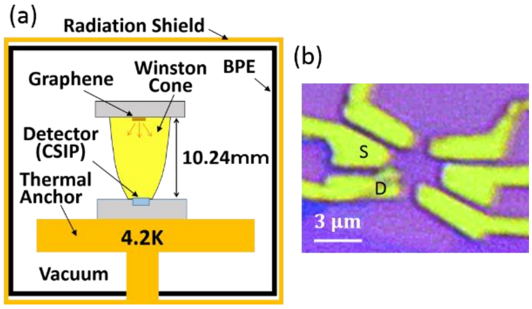


Fig. 1 (a) Schematic of the measurement setup. THz emission from graphene is focused on the CSIP through a Winston cone. (b) Optical micrograph of the graphene sample measured.

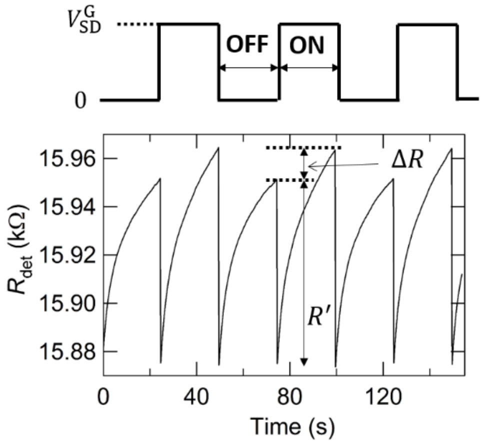


Fig. 2 Time trace of photoresponse at 4.43 T. The upper panel displays the 20 mHz modulation of the $V_{\mathrm{SD}}$ applied to the graphene device. The $R'$ and $\Delta R$ corresponds to photoresponse for background radiation and current-injected THz emission from graphene, respectively.

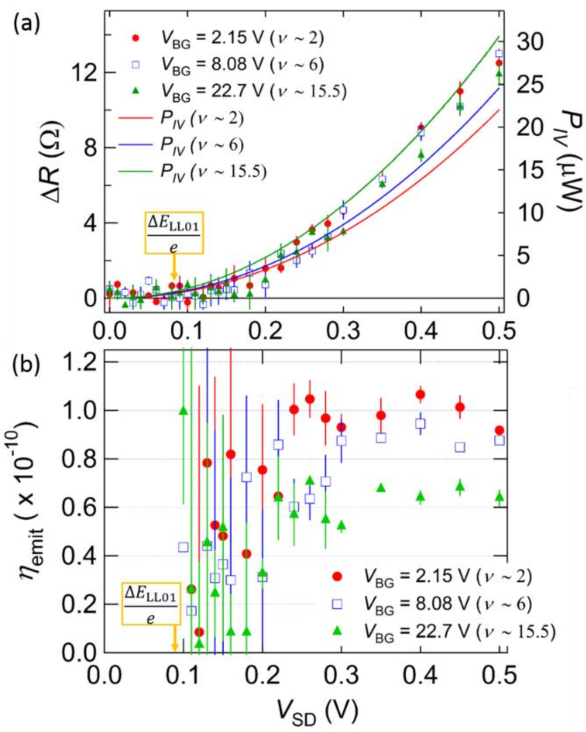


Fig. 3 (a) Photoresponse $\Delta R$ and electric power $P_{IV}$ applied to the graphene sample versus source-drain voltages $V_{SD}$ at 4.43 T. (b) Emission efficiency normalized by the $P_{IV}$ and background radiation power $P_B$.

14.5 μm and 9.1 μm). The detail layer structure and the spectrum have been described in Ref. [5]

The graphene LLs have an energy spectrum $E_N = \mathrm{sgn}(N) \times \sqrt{2e\hbar v_F^2 |N| B}$, where $e$ and $\hbar$ are electron charge and Planck's constant, and $v_F$ is the Fermi velocity of graphene. Using a value of $v_F = 1.118 \times 10^6$ [6], the LL energy spacing between the $N = 0$ and $N = +1$ states $\Delta E_{LL01}$ is magnetically tuned to a detectable wavelength of 14.5 μm at $B = 4.43$ T. It is confirmed that the current-injected emission from graphene is significantly reduced at $B = 6.9$ T (corresponds to the valley of the two-band spectrum of the CSIP) as well as at zero field. Background radiation, however, is larger than THz emission from graphene in this experiment setup. Thereby, the measurements of photoresponse have been performed by applying a 20 mHz-square wave to the source (S) and drain (D) contacts of the graphene sample (the upper panel of Fig.2). A typical time trace taken at a magnetic field $B = 4.43$ T is shown in Fig. 2. In an operating condition at 4.43 T, the resistance of the CSIP, $R_{det}$, increases at a rate proportional to the incident power, $P_{inc}$. The photoresponse of the current-injected emission, $\Delta R$, is obtained by subtracting the contribution of background radiation, $R'$.

## 3. Results and discussion

Figure 3(a) shows the $\Delta R$ versus the source-drain voltages $V_{SD}$ applied to the graphene sample. THz

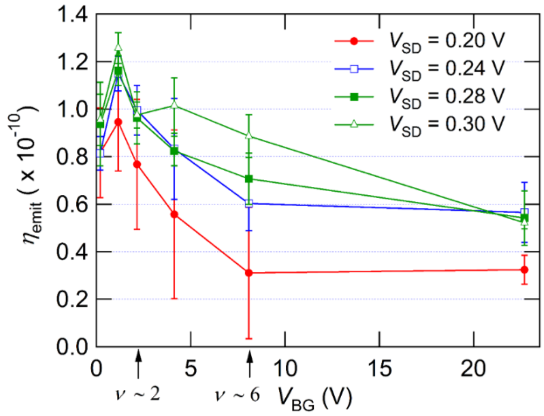


Fig. 4 Emission efficiency versus $V_{BG}$ at 4.43 T.

emission is definitely observed when the $eV_{SD}$ exceeds the LL energy spacing $\Delta E_{LL01}$. Since the resistance of graphene largely depends on the back-gate voltages $V_{BG}$ (namely, the LL filling factor $\nu$), we discuss the emission efficiency corrected by the applied electric power $P_{IV}$. The sensitivity of the detector at zero field is well characterized with a formula $P_{inc} = h\nu/(\eta_{det} \cdot \Delta I_e) \cdot (\Delta I_{sig}/\Delta t)$, where the photon energy $h\nu = 85.5$ meV, the detection efficiency $\eta_{det} = 0.17$, the photo-signal current induced by single-photon absorption, $\Delta I_e = 1.5$ pA [5]. Using an experimental value $\Delta I_{sig}/\Delta t = 410$ pA/s at zero field, background radiation incident to the photo-active area of the detector $P_B$ is estimated to be about $2.2 \times 10^{-17}$ W. The $\Delta R$ can be thus plotted as the emission efficiency $\eta_{emit} = 1/(\eta_{cone} \cdot P_{IV}) \times P_B \cdot (\Delta R/R')$, where $\eta_{cone}$ is the efficiency of the optical system with a Winston cone ($\eta_{cone} \approx 1.8 \times 10^{-3}$). As seen in Fig. 3(b) and Fig. 4, the $\eta_{emit}$ increases when the Fermi level is set to the energy between the $N = 0$ LL and $N = +1$ LL.

## 4. Conclusion

LL emission has been first observed by using a QW-based charge sensitive infrared phototransistor. The emission efficiency is enhanced when the $eV_{SD}$ exceeds the $\Delta E_{LL01}$ and the Fermi level is positioned between the $N = 0$ LL and the $N = +1$ LL, indicating the $N = +1 \to 0$ inter-LL radiative transition induced by electron injection.

## Acknowledgements

We acknowledge financial support from JSPS KAKENHI Grant Numbers 15K13496 and 25287071.

## References

[1] For instance, A. F. Young *et al.*, Nature **505**, 528 (2014)
[2] T. Kramer *et al.,* Phys. Rev. B **81**, 081410(R) (2010).
[3] K. Ikushima and S. Komiyama, C. R. Physique **11**, 444 (2010).
[4] S. Komiyama, IEEE J. Sel. Top. Quantum Electron. **17**, 54 (2011).
[5] S. Kim *et al*., Appl. Phys. Lett. **107**, 182106 (2015).
[6] R. S. Deacon *et al*., Phys. Rev. B **76**, 081406(R) (2007).